

Electronic Supplementary Information

Covalent organic framework based nanoagent for enhanced mild-temperature photothermal therapy

Qiaoqiao Sun[†], Kun Tang[†], Liqun Song, Yanhua Li, Wei Pan, Na Li* and Bo Tang*

College of Chemistry, Chemical Engineering and Materials Science, Key Laboratory of Molecular and Nano Probes,
Ministry of Education, Collaborative Innovation Center of Functionalized Probes for Chemical Imaging in
Universities of Shandong, Institute of Molecular and Nano Science, Shandong Normal University, Jinan 250014, P.
R. China.

E-mail: lina@sdu.edu.cn; tangb@sdu.edu.cn

Table of Contents

1. Experimental Procedures	S3
1.1 Materials and Instruments	S3
1.2 Cell culture and animal model	S3
2. Supplementary Figures	S4
Figure S1	S4
Figure S2	S4
Figure S3	S4
Figure S4	S5
Figure S5	S5
Figure S6	S5
Figure S7	S6
Figure S8	S6
Figure S9	S7
Figure S10	S7
Figure S11	S8
Figure S12	S8
Figure S13	S9
Figure S14	S9

1. Experimental Procedures

1.1 Materials and instruments. Gambogic acid were purchased from Shanghai Aladdin Biochemical Technology Co., Ltd., China. Dimethyl sulfoxide was purchased from China National Pharmaceutical Group Corporation (Shanghai, China). Fetal bovine serum (FBS) was purchased from Gibco, USA. RPMI 1640 medium was purchased from Nanjing Key Gen Biotech. Co., Ltd., China. Calcein-AM/PI Double Stain Kit were purchased from Beyotime (Nantong, China). 3-(4,5-dimethylthiazol-2-yl)-2,5-diphenyltetrazolium bromide (MTT) were purchased from Sigma Chemical Company. 96-well plates were purchased from Hangzhou Xinyou Biotechnology Co., Ltd, China. 4T1 cell were purchased from Procell Life Science&Technology Co., Ltd, China. All the aqueous solutions used in experiments were prepared using deionized water (18.2 M Ω cm) obtained from a Milli-Q water purification system. All chemicals were of analytical grade and were used without further purification. Fourier infrared spectrometer (Nicolet iS50 FT-IR) was used to characterize the infrared spectrum. Powder X-ray diffraction (XRD) pattern was carried out on a Rigaku SmartLab SE X-Ray Powder Diffractometer with Cu K α line focused radiation ($\lambda = 1.5405 \text{ \AA}$). Transmission electron microscopy (TEM) was obtained on a JEM-100CX II electron microscope. UV-Vis absorption spectra were measured on pharماسpec UV-1700 UV-Visible spectrophotometer (Shimadzu, Japan). Absorbance was measured in a microplate reader (Synergy 2, Biotek, USA) in the MTT assay. Success of each reaction step was confirmed by monitoring the changes in zeta potential with a Malvern Zeta Sizer Nano (Malvern Instruments). Confocal fluorescence imaging assay were performed with a TCS SP8 confocal laser scanning microscopy (Leica, Germany). Western Blotting was performed by ChemiDoc XRS gel imaging system (bio-rad, Hercules, CA, USA). The in vivo imaging study was performed with a Caliper IVIS Lumina III imaging system (Caliper Co., USA).

1.2 Cell culture and animal model. The mouse breast cancer cell line (4T1) was cultured in RPMI 1640 medium supplemented with 10% fetal bovine serum (FBS) and 100 U/mL 1% antibiotics penicillin/streptomycin. The cells were grown at 37 °C under 5% CO₂ in a humidified cell incubator. The healthy breast cells (MCF-10A) were cultured in MCF-10A special medium containing 10% FBS and 100 U/mL of 1% antibiotics (penicillin/streptomycin) and were maintained at 37 °C in a 5% CO₂/95% air humidified incubator (SANYO).

Balb/c mice were reviewed and approved by the Ethics Committee of Shandong Normal University, Jinan, P. R. China. All the animal experiments were conducted under relevant guidelines of the Chinese government and regulations for the care and use of experimental animals.

2. Supplementary Figures

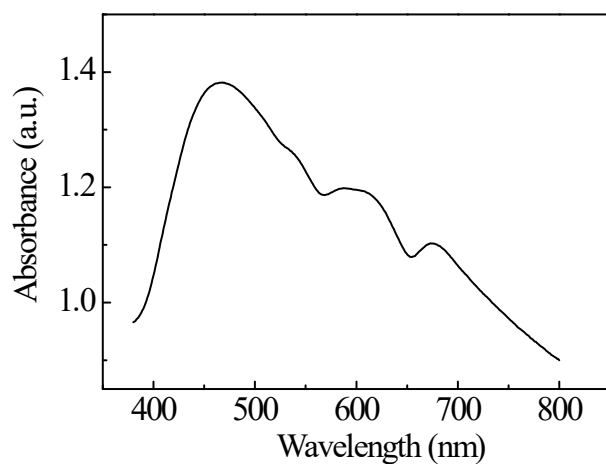


Figure S1. UV-Vis adsorption spectra of COFs.

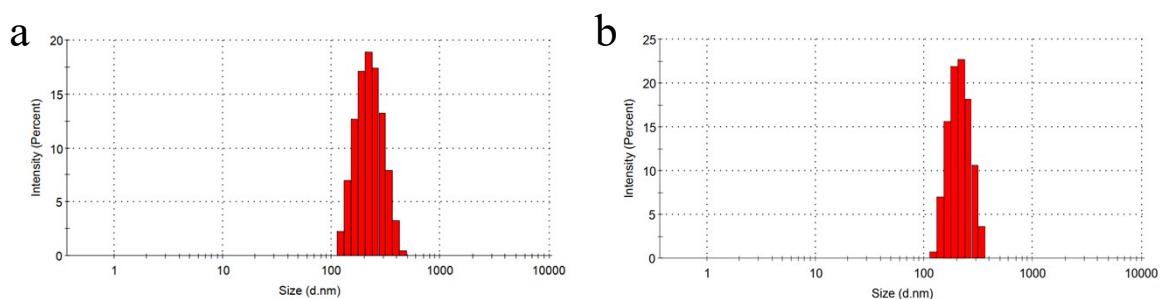


Figure S2. DLS-measured hydrodynamic sizes of (a)COFs and (b)COF-GA.

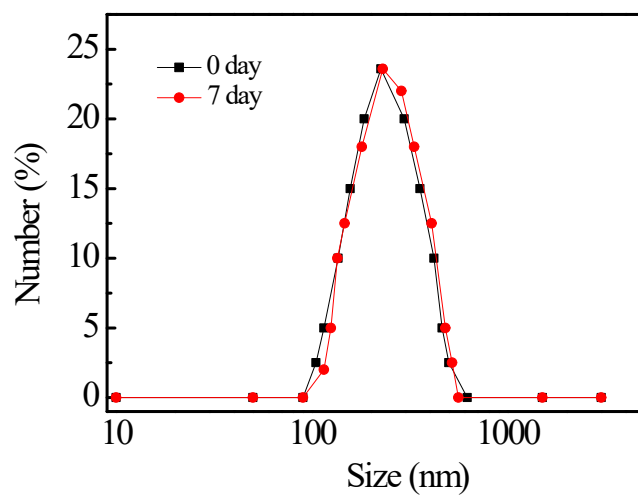


Figure S3. DLS-measured hydrodynamic sizes of COF-GA with various time in PBS.

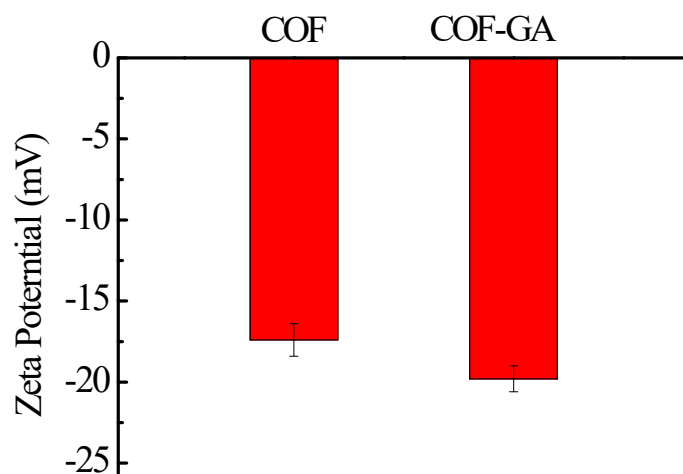


Figure S4. Zeta potential of COFs and COF-GA.

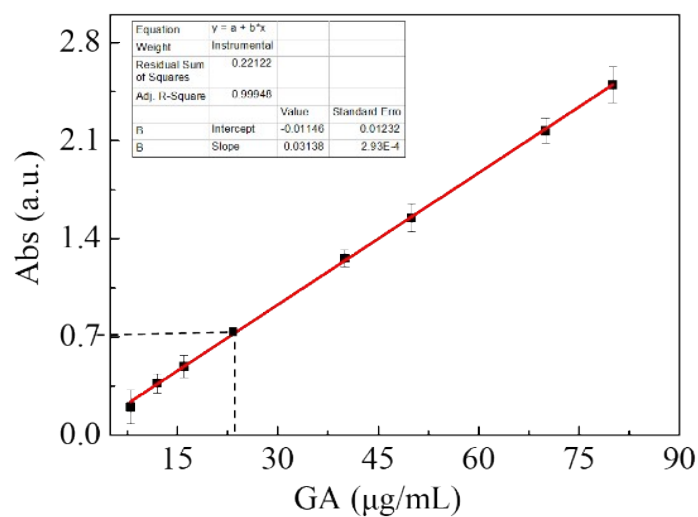


Figure S5. The standard curve of GA was measured by nanodrop. The absorbance of the supernatant was measured as 0.73, the concentration of GA was 23.63 $\mu\text{g/mL}$.

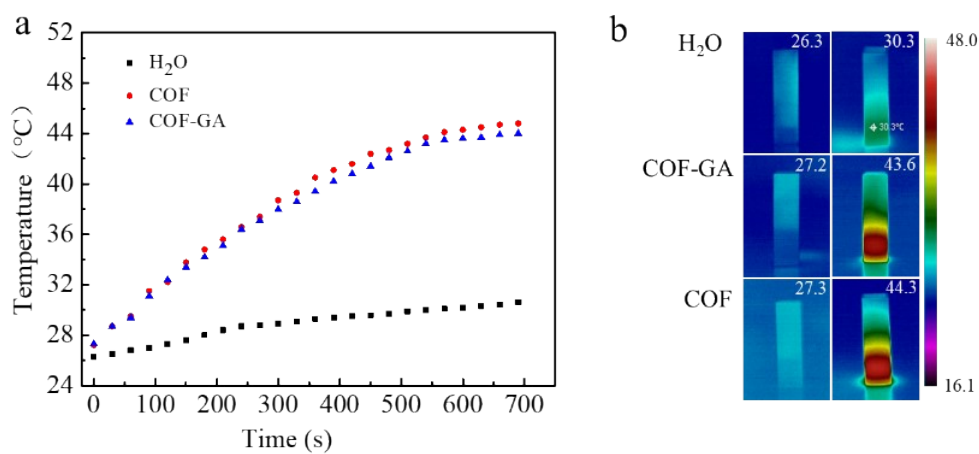


Figure S6. (a) Temperature variation curves for H₂O, COF and COF-GA with the concentrations of 100 $\mu\text{g/mL}$ under laser irradiation (635 nm, 0.3 W/cm²). (b) Photothermal images of H₂O, COF and COF-GA in solution before and after laser.

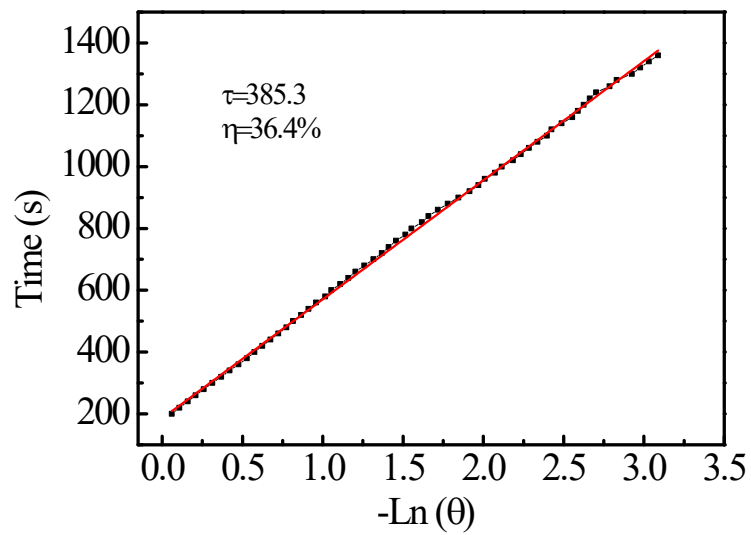


Figure S7. Linear correlation of the cooling times versus negative natural logarithm of driving force temperatures.

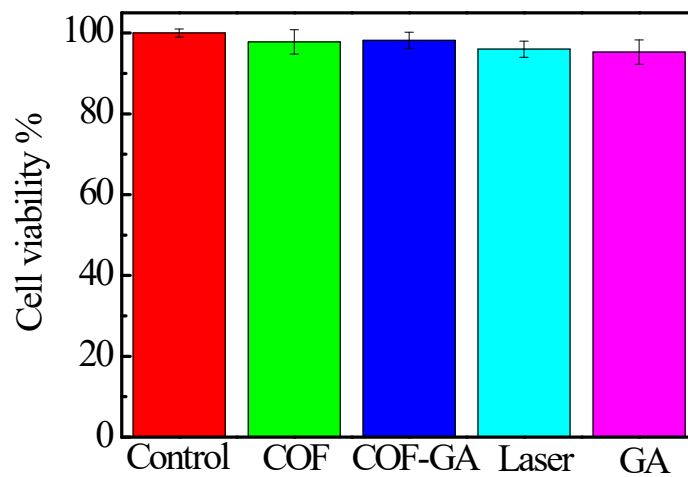


Figure S8. Cell viability of MCF-10A cells incubated with, COF, COF-GA, Laser and GA. The laser irradiation was 635 nm, 0.3 W/cm² for 10min.

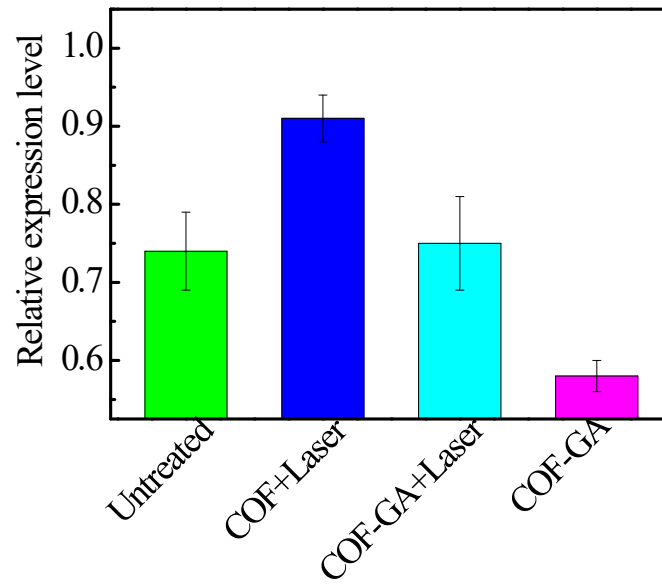


Figure S9. Relative HSP90 expression levels of cells after various treatments.

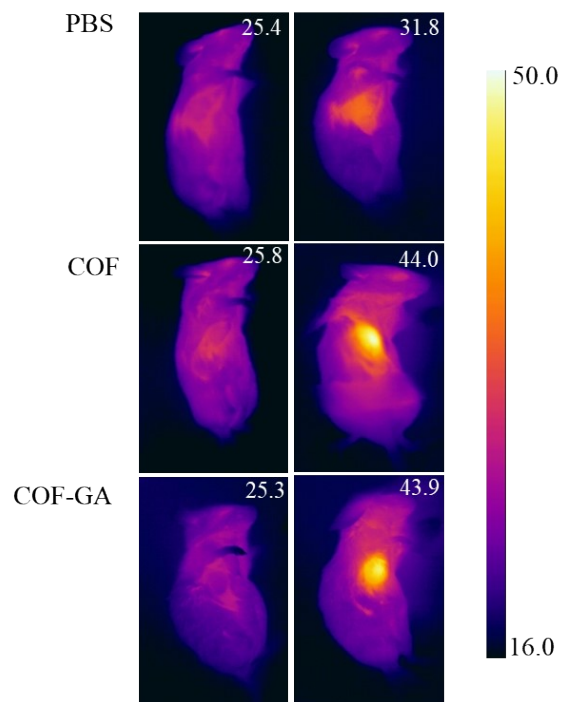


Figure S10. Thermal images of 4T1 tumor-bearing mice exposed to laser irradiation at 0.3 W/cm² power for 10 min after intratumorally injection of PBS, COF and COF-GA.

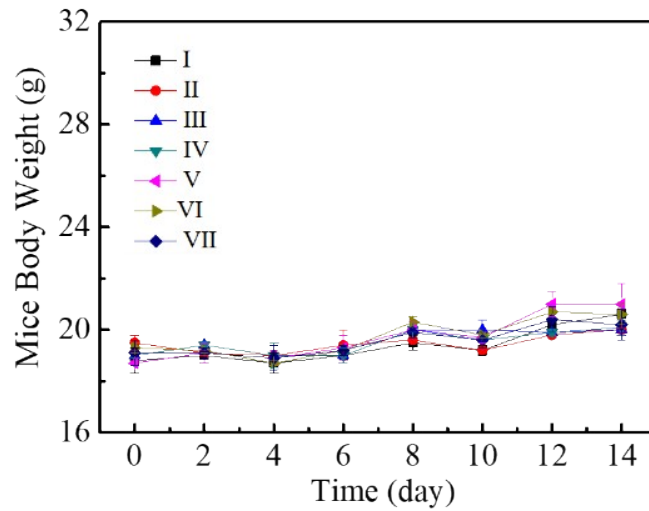


Figure S11. Body weight curves of mice with different treatments.

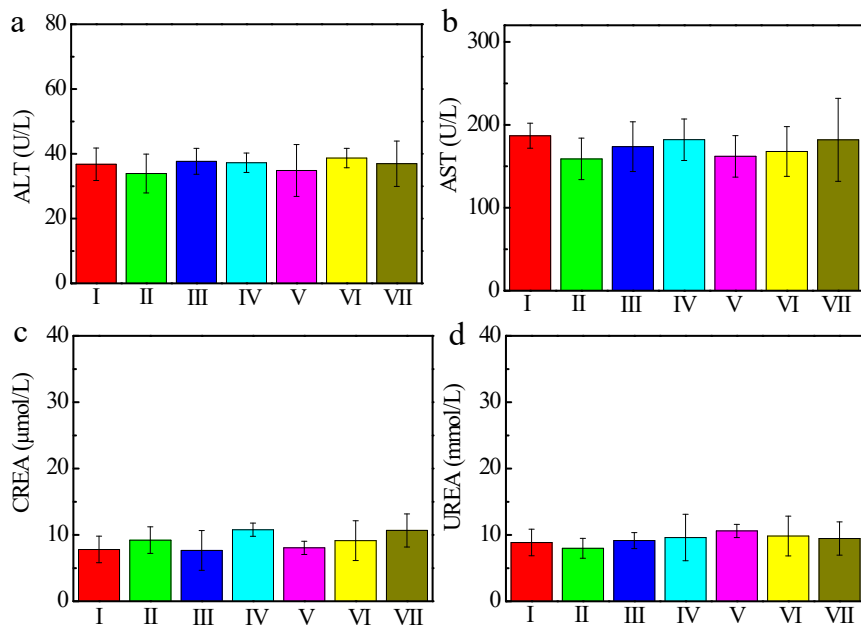


Figure S12. Blood biochemical tests (ALT, AST, CREA and UREA) of Balb/C mice after treatments. (I) PBS; (II) COF; (III) COF-GA; (IV) Laser; (V) GA; (VI) COF+Laser; (VII) COF-GA+Laser.

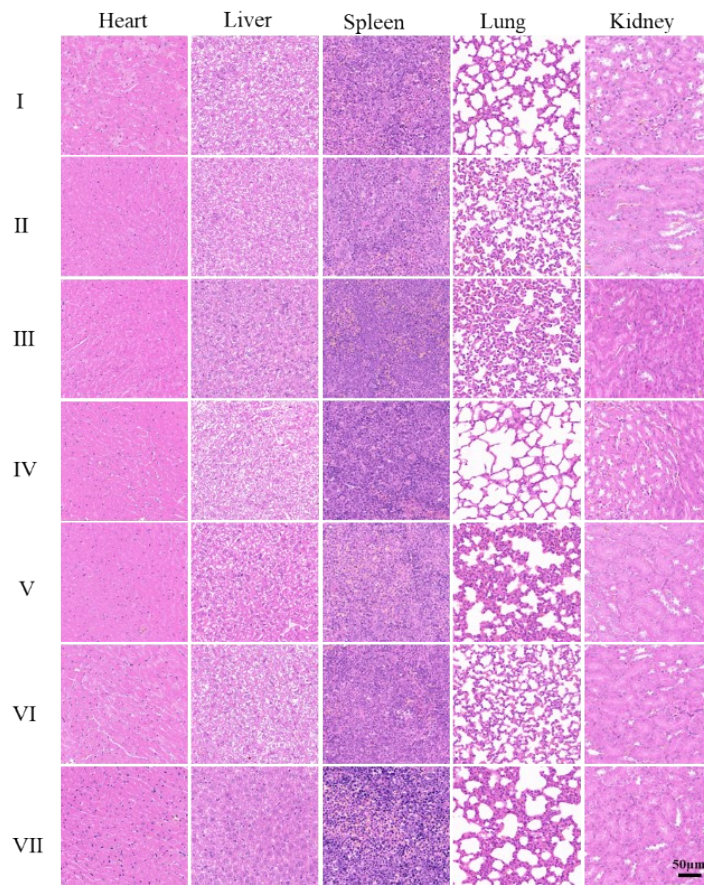


Figure S13. H&E staining images of major organs (heart, liver, spleen, lungs, and kidneys).

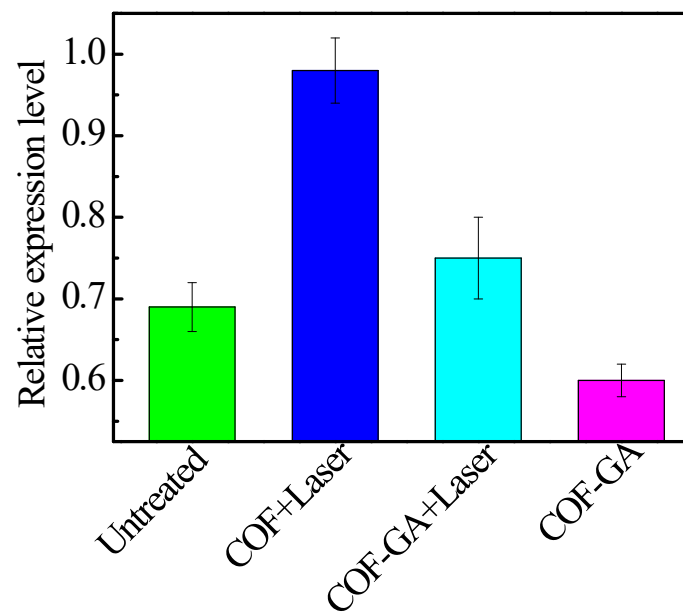


Figure S14. Relative HSP90 expression levels of tumors after various treatments.